Thermodynamic modeling and experimental study of alkali-activated slag paste

Zuo, Yibing; Nedeljkovic, Marija; Arbi Ghanmi, Kamel; Ye, Guang

Publication date
2016

Document Version
Accepted author manuscript

Published in
Ultra-high performance concrete and high performance construction materials

Citation (APA)
Zuo, Y., Nedeljkovic, M., Arbi Ghanmi, K., & Ye, G. (2016). Thermodynamic modeling and experimental study of alkali-activated slag paste. In E. Fehling, B. Middendorf, & J. Thiemicke (Eds.), *Ultra-high performance concrete and high performance construction materials: Proceedings of HiPerMat 2016, Kassel, Germany* (27 ed., Vol. 27, pp. 1-8). Kassel University Press.

Important note
To cite this publication, please use the final published version (if applicable).
Please check the document version above.

THERMODYNAMIC MODELING AND EXPERIMENTAL STUDY OF ALKALI-ACTIVATED SLAG PASTE

Yibing Zuo, Marija Nedeljkovic, Kamel Arbi, Guang Ye
Faculty of Civil Engineering and Geosciences, Delft University of Technology, The Netherlands

Abstract: A newly developed thermodynamic approach was introduced from the literature to investigate the influence of NaOH content on the hydrate assemblage and chemistry of aqueous solution of activated slag paste (Na_2O/slag=4%, 6% and 8%). The ICP-OES test was performed to obtain the aqueous species profiles such as Si, Ca, Al and Na etc. The elemental concentrations in aqueous solution show a similar trend between thermodynamic calculations and experimental results. The modeling results showed that the influence of NaOH content on the uptake of Na into the primary reaction products and chemical shrinkage depends on slag reaction extent and NaOH content. The NaOH content does not show an obvious influence on the porosity development. The volume fraction of primary products in total products is between 40% and 60%, and particularly increases slightly after a certain degree of reaction for activated slag with Na_2O/slag=4% and 6%. The volume ratio between total products and reacted slag is around 1.5~1.7, smaller than the value from 2.06 to 2.2 reported for Portland cement.

Keywords: thermodynamic modeling, NaOH, slag, pore solution, chemical shrinkage

1 Introduction

Thermodynamics is essential to the understanding of chemical reactions, which enables the prediction if a reaction will take place and the calculations of the stable phase assemblage and the aqueous phase composition at the final state once the reaction is completed. The thermodynamic modelling has been extensively and successfully used in the research of hydration in Portland cement-based materials. [1, 2] However, the thermodynamic equilibrium calculations are not popularly used in the research of alkali-activated materials. The limited utilization of thermodynamic modelling in the hydration of alkali-activated slag is mainly due to the insufficient data on the solubility products of the primary reaction products. Because of the amorphous nature of the primary reaction products and the complex chemical environments in alkali-activated slag, there are few experimental researches carried out for alkali-activated slag cement to determine these thermodynamic data including chemical reactions and thermodynamic equilibrium constants.

Lothenbach and Gruskovnjak [3] used a solid solution model developed by Kulik and Kersten [4] to simulate the primary binding gels in the alkali-activated slag systems. In their approach, the primary binding gel is described as a system of two concurrent solid solution systems, based on which the uptake of Al was considered using Al/Si ratio of 0.1 and the uptake of alkalis considered very roughly using a distribution ratio of alkali between primary binding gel and the aqueous solution. Their calculation results showed the composition of the pore solution and the assemblage of reaction products agreed with the observed composition in the different alkali-activated systems.

However, for thermodynamic modelling the ability to formally account for the uptake of Al and Na into the primary reaction products is of great significance. Myers et al. for the first time proposed a thermodynamic approach to account explicitly for the structurally-incorporated Al and Na species in the primary reaction products, C-(N)-A-S-H gel, and apply it to simulate the chemistry of primary reaction products in alkali-activated slag cement. [5] In this approach, they used a minimal set of eight end-members to describe the primary reaction products based on the sublattice solid solution model and estimated the thermodynamic properties through the optimization of the solubility products for the dissociation reactions of these eight-members. The

uptake of Al and Na were considered as independent substitution of tetrahedral Al and Na species in the formation. This derived thermodynamic model was used to describe solubility data for sodium silicate and sodium carbonate activated slag and chemical composition data for the primary binding gels. [5, 6] However, the NaOH activated slag was not thermodynamically modelled in detail regards to hydrate assemblage and chemistry of aqueous solution.

This paper introduced the thermodynamic model developed by Myers et al. to investigate the influence of sodium hydroxide content on the hydrate assemblage and chemistry of aqueous solution of NaOH activated slag paste. In the meanwhile, inductively coupled plasma-optical emission spectroscopy (ICP-OES) test was performed to study the elemental concentration of aqueous solution in the NaOH activated slag paste.

2 Materials and methods

Materials and mixtures

The chemical composition of blast furnace slag listed in Table 1 was determined by X-ray fluorescence spectrometry (XRF). Sodium hydroxide (analytical grade, >98%) was mixed with distlled water to formulate activating solution. Three contents of sodium hydroxide were selected with Na_2O/slag =4%, 6% and 8%. For all the mixtures the water/slag ratio was fixed at 0.4. These three mixtures were denoted as Na_2O_4%, Na_2O_6% and Na_2O_8% corresponding to the mixtures with Na_2O/slag =4%, 6% and 8% respectively.

Table 1: Chemical composition of blast furnace slag.

Oxide		SiO_2	CaO	Al_2O_3	MgO	Fe_2O_3	SO_3	K2O	TiO_2	L.I.
Weight	%	32.91	40.96	11.85	9.23	0.46	1.61	0.33	1.00	1.15

ICP-OES test

The slag and activating solution were mixed in a commercial Hobart mixer with two minutes low-speed and subsequently two-minutes high speed mixing. Then the mixed slag paste was cast in commercial cylinder polyethylene jars (d=35 mm and h=70 mm) and vibrated for 30 seconds on a vibrating table. All the specimens were stored in the closed jars in the curing room at room temperature and with the relative humidity about 100% until the testing age.

The pore solution of the specimens were extracted following the procedures described by Barneyback and Diamond [7] at the age of 3 h, 7h, 12 h, 1 d, 3 d, 7 d, 14 d and 28 d. Pressures of up to 300 MPa were used to express pore fluid from the samples at different ages. After extraction, the pore solution was immediately filtered using Whatman 41 filter paper and then divided into two equalling parts. The filtered solution were diluted using nitric acid (0.2 vol.%) and the diluted solutions were analysed through a VARIAN Vista 720 ICP-OES spectrometer. After ICP-OES test, the residual filtered solution was used to measure the concentration of OH^- through titration against hydrochloric acid (0.1 mol/L).

Thermodynamic modelling

The thermodynamic model assumes a thermodynamic equilibrium between the aqueous species in the pore solution and the precipitating reaction products, based on which the reaction products and the concentrations of aqueous species in the pore solution can be calculated. The newly developed thermodynamic approach by Myers et al. [5] was introduced in this paper. The chemical reactions and corresponding thermodynamic properties of the eight end-members were reproduced in Table 2. In the calculations of Myers et al., Fe was not considered due to its very low content in slag and sulfur was represented as S^{2-}. According to Wolthers et al., [8], disordered mackinawite is the first iron sulfid to form in most ambient environments, and with time it reacts to form more stable iron sulfid phases such as ordered mackinawite and ultimately pyrite or pyrrhotite. Lothenbach and Gruskovnjak reported that mackinawite is more stable in

the alkali-activated slag system than other phases lilke Fe-ettringite or microcrystalline $Fe(OH)_3$. [3] Therefore mackinawite was included in this paper to consider the reactions between aqueous Fe^{2+} and S^{2-} under ambient conditions. More details on the thermodynamic properties of other secondary reaction products can be refered to [6].

Table 2: Chemical reactions and equilibrium constants at 25℃ and 1 bar for eight end-members.[5]

End-member	Chemical reactions	*Log K*
5CA	$(CaO)_{1.25}\cdot(Al_2O_3)_{0.125}\cdot(SiO_2)\cdot(H_2O)_{1.625} \Leftrightarrow 1.25Ca^{2+} + SiO_3^{2-} + 0.25AlO_2^- + 0.25OH^- + 1.5H_2O$	-10.75
INFCA	$(CaO)\cdot(Al_2O_3)_{0.15625}\cdot(SiO_2)_{1.1875}\cdot(H_2O)_{1.65625} + 0.6875OH^- \Leftrightarrow Ca^{2+} + 1.1875SiO_3^{2-} + 0.3125AlO_2^- + 2H_2O$	-8.90
5CNA	$(CaO)_{1.25}\cdot(Na_2O)_{0.25}\cdot(Al_2O_3)_{0.125}\cdot(SiO_2)\cdot(H_2O)_{1.25} \Leftrightarrow 1.25Ca^{2+} + SiO_3^{2-} + 0.25AlO_2^- + 0.5Na^+ + 0.75OH^- + H_2O$	-10.40
INFCNA	$(CaO)\cdot(Na_2O)_{0.34375}\cdot(Al_2O_3)_{0.15625}\cdot(SiO_2)_{1.1875}\cdot(H_2O)_{1.3} \Leftrightarrow Ca^{2+} + 1.1875SiO_3^{2-} + 0.3125AlO_2^- + 0.6875Na^+ + 1.3125H_2O$	-10.00
INFCN	$(CaO)\cdot(Na_2O)_{0.3125}\cdot(SiO_2)_{1.5}\cdot(H_2O)_{1.1875} + 0.375OH^- \Leftrightarrow Ca^{2+} + 1.5SiO_3^{2-} + 0.625Na^+ + 1.375H_2O$	-10.70
T2C*	$(CaO)_{1.5}\cdot(SiO_2)\cdot(H_2O)_{2.5} \Leftrightarrow 1.5Ca^{2+} + SiO_3^{2-} + OH^- + 2H_2O$	-11.60
T5C*	$(CaO)_{1.25}\cdot(SiO_2)_{1.25}\cdot(H_2O)_{2.} \Leftrightarrow 1.25Ca^{2+} + 1.25SiO_3^{2-} + 2.5H_2O$	-10.50
TobH*	$(CaO)\cdot(SiO_2)_{1.5}\cdot(H_2O)_{2.5} + OH^- \Leftrightarrow Ca^{2+} + 1.5SiO_3^{2-} + 3H_2O$	-7.90

Simulations for the three mixtures were carried out in an N_2 atmosphere at 25 ℃, 1 bar using GEM-Selektor V3. [9, 10] Congruent slag dissolution was assumed and proportional additions of SiO_2, CaO, Al_2O_3, MgO, Fe_2O_3, H_2S and K_2O were used to simulate the slag reaction extents and bulk chemical composition. Usually the slag contains more than 95% vitreous phase. [11] Considering the impurities of slag, this study takes SiO_2, CaO, Al_2O_3, MgO, Fe_2O_3, H_2S and K_2O to be fully dissolved and reacted in the modelling. It is worth noting that the samples were cured at 20 ℃ during the ICP-OES test, which is slightly different from the standard equilibrium temperature. However, this difference does not have a significant influence on the rate of diffusion or the stability of minerals, [12], and hence would not impose a significant impact on the equilibrium constants and the thermodynamic modelling results.

3 Results and discussion

Chemical composition of aqueous solution through ICP-OES test and simulation

Figures 1-3 show the concentrations of elements in the aqueous solution through ICP-OES test and thermodynamic modelling. The dashed vertical lines corresponding to the curing time were estimated from the literatures. [13] The experimental and simulation results both indicate that the pore solution of NaOH activated slag systems were initially dominated by Na and OH^- that are dissolved from the activator and increase with increasing content of Na_2O from 4% to 8% and decrease gradually with slag reaction. Contrary to Na, the concentration of K increases. This is because the K comes from slag and increases with slag dissolution while Na decreases as it is taken up by primary reaction products. [3] The concentration of Ca remains at a very low level and does not show an obvious change during the slag reaction process, which is due to the low solubility of Ca in high alkalinity environment indicated by the high concentration of OH^-. The concentrations of Si and Al decrease with progress of slag reaction as they react to form reaction products. On the other hand the NaOH content increases the concentrations of Si and Al as high alkalinity accelerates the dissolution of slag.

Through the comparison between experimental and simulation results, it can be seen that the calculated concentrations of elements in the aqueous solution agree well with the testing results particularly in terms of Na, OH^-, Ca, Si and Al, indicating reliable results obtained from

thermodynamic modelling. Besides the profiles of these elements detected by experimental study, the thermodynamic calculations also give the concentrations of Mg and Fe that were under the measurement limit of ICP-OES test. The concentration of Mg is lower than Ca by the number of 6 magnitudes, which suggests rapid formation of OH-hydrotalcite during the slag reaction. The concentration of Fe decreases as it reacted with S to form mackinawite.

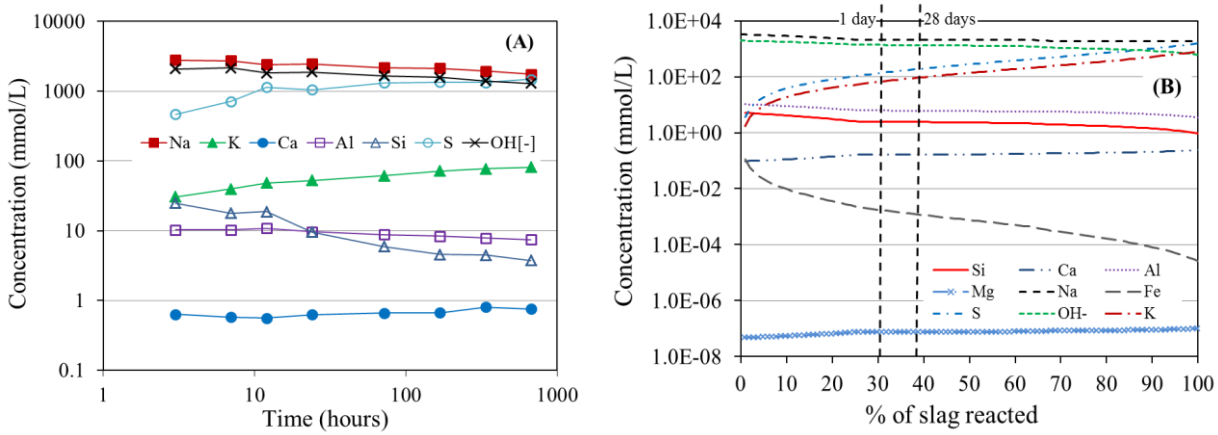

Figure 1: Elemental concentrations of aqueous solution through test (A) and simulation (B) for Na_2O_4%.

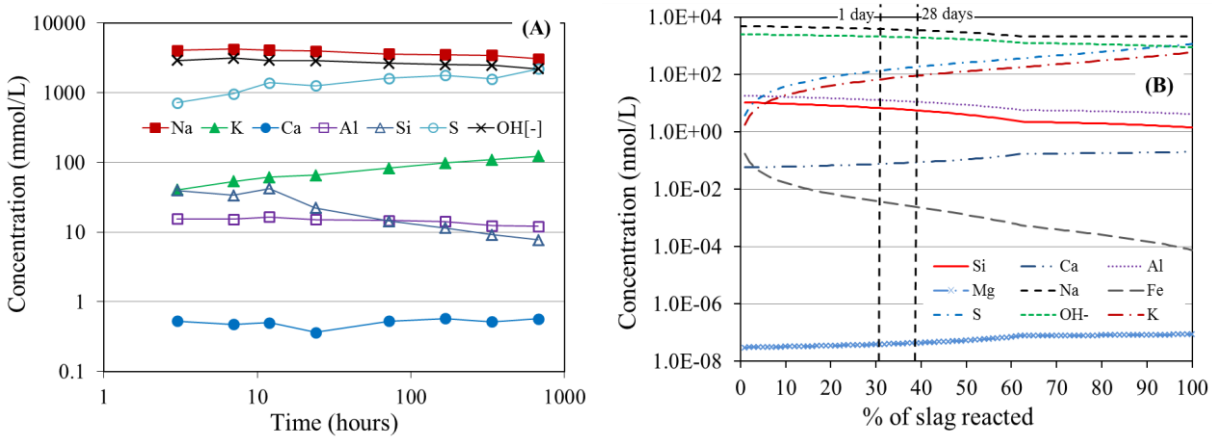

Figure 2: Elemental concentrations of aqueous solution through test (A) and simulation (B) for Na_2O_6%.

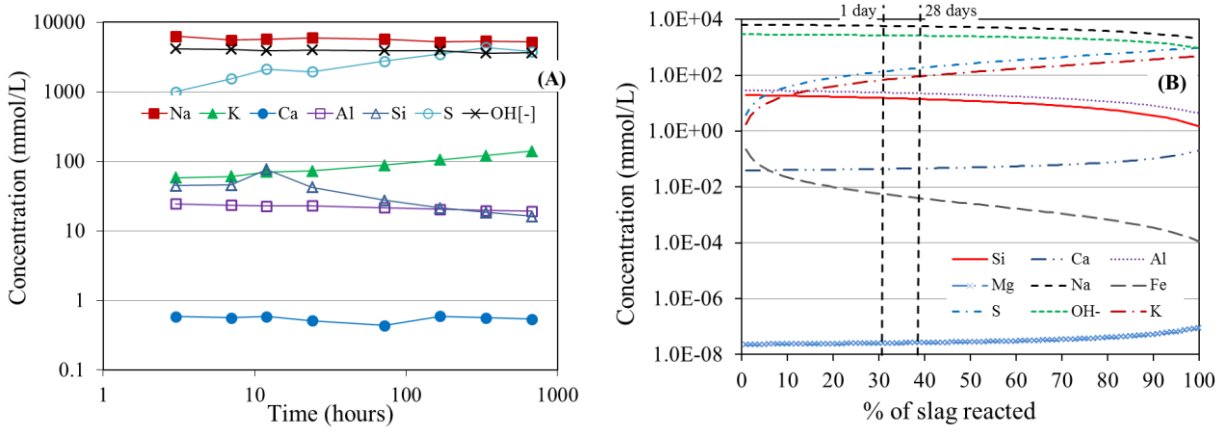

Figure 3: Elemental concentrations of aqueous solution through test (A) and simulation (B) for Na_2O_8%.

Simulated phase assemblage through thermodynamic modeling

The calculated primary products as well as the secondary products in volume and mole quantities were plotted as a function of slag reaction extent in Figures 4-6 for Na_2O_4%, Na_2O_6% and Na_2O_8% respectively. Here the chemical shrinkage is defined as the volume reduction between initial total volume of slag and activating solution and the total volume of unreacted slag, reaction products and aqueous solution after slag reaction. Because of the

impurity of the slag, the volume of unreacted slag is not zero when slag reaches 100% reaction extent as shown in Figures 4-6.

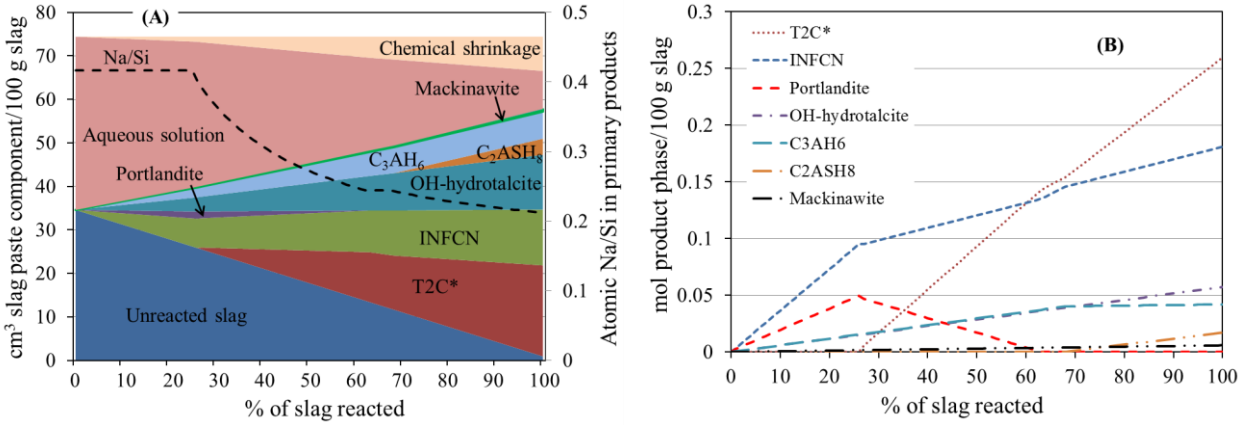

Figure 4: Calculated reaction products in volume (A) and mol (B) quantities/100 g slag for Na_2O_4%.

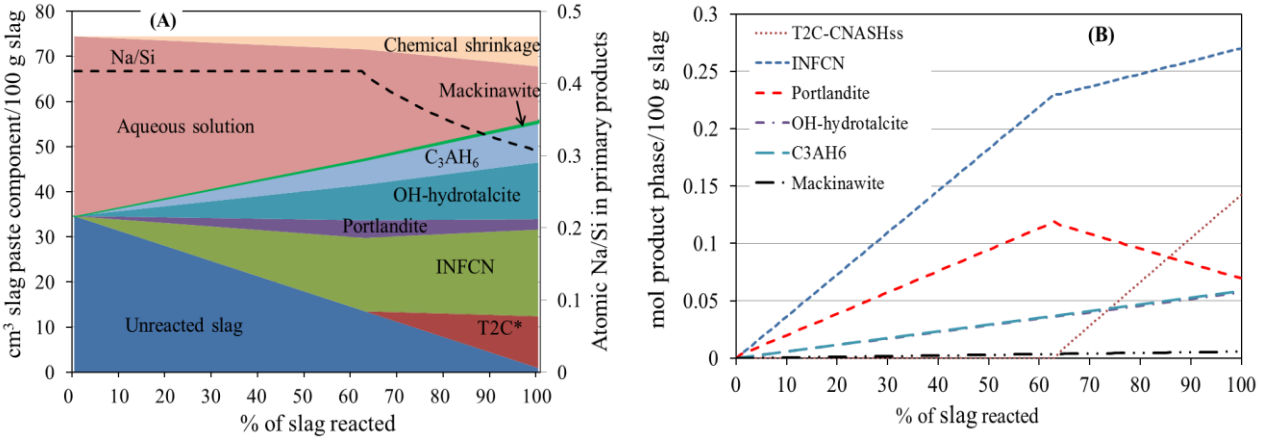

Figure 5: Calculated reaction products in volume (A) and mol (B) quantities/100 g slag for Na_2O_6%.

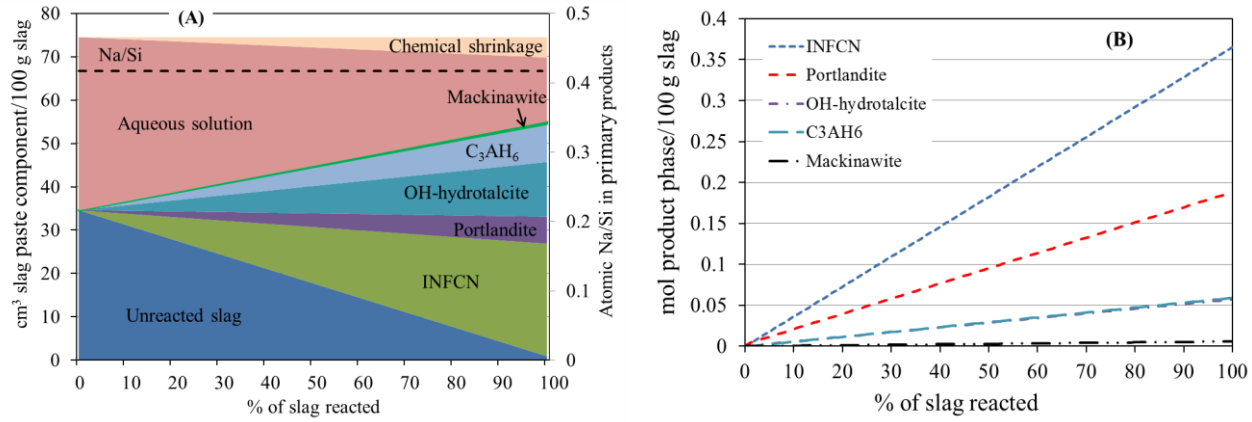

Figure 6: Calculated reaction products in volume (A) and mol (B) quantities/100 g slag for Na_2O_8%.

Eight end-members as listed in Table 2 were used to simulate the primary products of alkali-activated slag cement with independent uptake of Al and Na. Figures 4-5 shows that only T2C*, a C-S-H gel end-member, and INFCN, a C-N-S-H gel end-member, were produced for Na_2O_4% and Na_2O_6%; with increasing Na_2O from 4% to 6%, the production of T2C* is delayed and reduced. When Na_2O was increased to 8%, only INFCN was produced for Na_2O_8% during the whole slag reaction process. It indicates that increasing NaOH content increases uptake of Na into primary products after a certain slag reaction extent. This characteristic can also be reflected by the atomic Na/Si ratio in primary products as plotted in Figures 4(A)-6(A). For Na_2O_4% and Na_2O_6%, Na/Si is 0.417 in the beginning period and starts to decrease with increasing slag reaction extent after T2C* was produced. As increasing Na_2O from 4% to 6%, the Na/Si decreases more slowly. When Na_2O was increased to 8%, Na/Si ratio remains

constant at 0.417 during the whole slag reaction process. Among the eight end-members as illustrated in Table 2, 5CA and INFCA, two C-A-S-H gel end-members, 5CNA and INFCNA, two C-N-A-S-H gel end-members, were used to describe the uptake of Al into the primary products. However, there were no such end-members produced in the calculation results as seen from Figs. 4-6. It seems that for NaOH activated slag with Na_2O/slag=4%, 6% and 8% in this study, Al were entirely incorporated into secondary reaction products.

Many secondary reaction products were considered and included in the thermodynamic calculations. It can be seen from Figures 4-6 that OH-hydrotalcite and katoite (C_3AH_6) are the main secondary reaction products and stratlingite (C_2ASH_8), mackinawite and portlandite are the minor secondary reaction products. The production of main secondary reaction products and mackinawite increased with slag reaction extent and were found independent of the NaOH content. Stratlingite was only produced for Na_2O_4%. The production of portlandite increased with increament of Na_2O from 4% to 8%. When Na_2O/slag=4%, portlandite was produced before slag reaction extent of 60% and afterwards it disappeared as shown in Figure 4.

The chemical shrinkage (cm^3/g slag) and porosity were plotted as a function of slag reaction extent in Figure 7(A) and Figure 7(B) respectively for Na_2O_4%, Na_2O_6% and Na_2O_8%. Here the porosity refers to the volume fraction of total volume of aqueous solution and chemical shrinkage in the total volume of all components as shown in Figures 4-6.

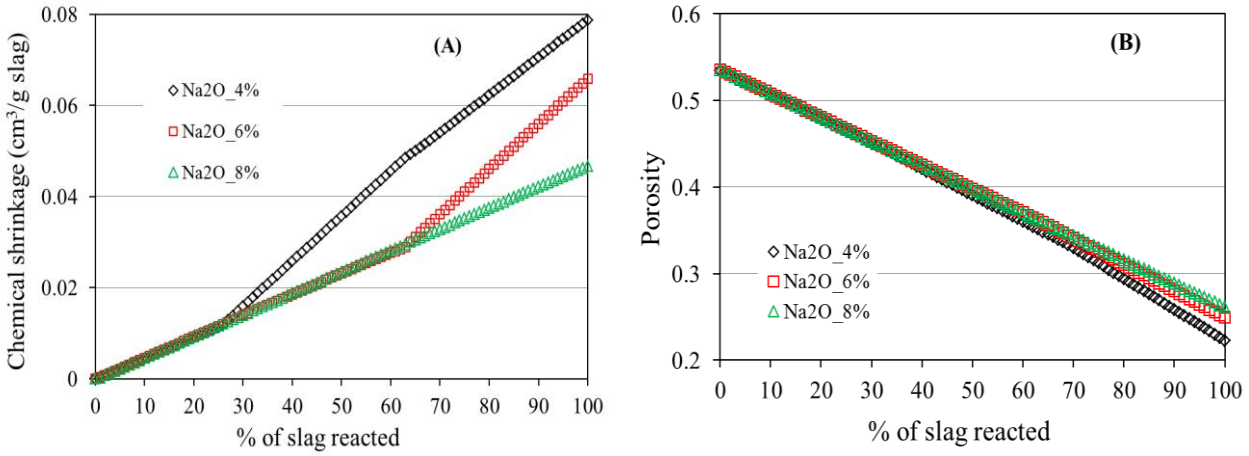

Figure 7: Volume fraction of chemical shrinkage (A) and porosity (B).

As seen in Figure 7(A), the chemical shrinkage is independent of Na_2O content from 4% to 8% before slag reaction extent of 28%, and independent of Na_2O content from 6% to 8% before slag reaction extent of 64%. After 28%, the chemical shrinkage of Na_2O_4% starts to increase more quickly and after 64%, it decreases with increasing Na_2O content from 4% to 8%. For Na_2O_8%, the chemical shrinkage has a quasi-linear relationship with the slag reaction extent. When slag reaction extent reaches 100%, the chemical shrinkage is 0.079, 0.066 and 0.047 cm^3/g slag for Na_2O_4%, Na_2O_6% and Na_2O_8% respectively, different from the value of 0.064 cm^3/g cement reported for Portland cement when cement completely hydrated. [14] This characteristic indicates that the chemical shrinkage per gram of reacted slag is dependent on the activator used for alkali-activated slag cement. When it was expressed in volume fraction, the chemical shrinkage is 0.106, 0.088 and 0.063 for Na_2O_4%, Na_2O_6% and Na_2O_8% respectively. The value of 0.106 for Na_2O_4% is different from the value of 0.15 reported for sodium silicate activated slag (Na_2O/slag=4%, water/slag=0.4) when slag completely reacted. [15] This difference was due to high polymerization degree caused by the higher alkalinity of NaOH than silicate activator. The increased polymerization degree due to increased alkalinity reduces water consumption and as a result reduces chemical shrinkage.

Figure 7(B) shows that the porosity of NaOH activated slag decreases with increasing slag reaction extent, and was found independent of Na_2O content from 4% to 8% until slag reaction

extent of 75%. After 75%, the porosity increases very slightly with increasing NaOH content, but still very close to each other for Na_2O_4%, Na_2O_6% and Na_2O_8%. Therefore the content of NaOH does not have an obvious influence on the porosity development of alkali-activated slag.

Solid phase growth

The volume fraction of primary reaction products ($V_{p\_products}$) in total reaction products ($V_{products}$) and the volume ratio between reaction products ($V_{products}$) and reacted slag ($V_{s\_reacted}$) were plotted in Figure 8 for Na_2O_4%, Na_2O_6% and Na_2O_8%.

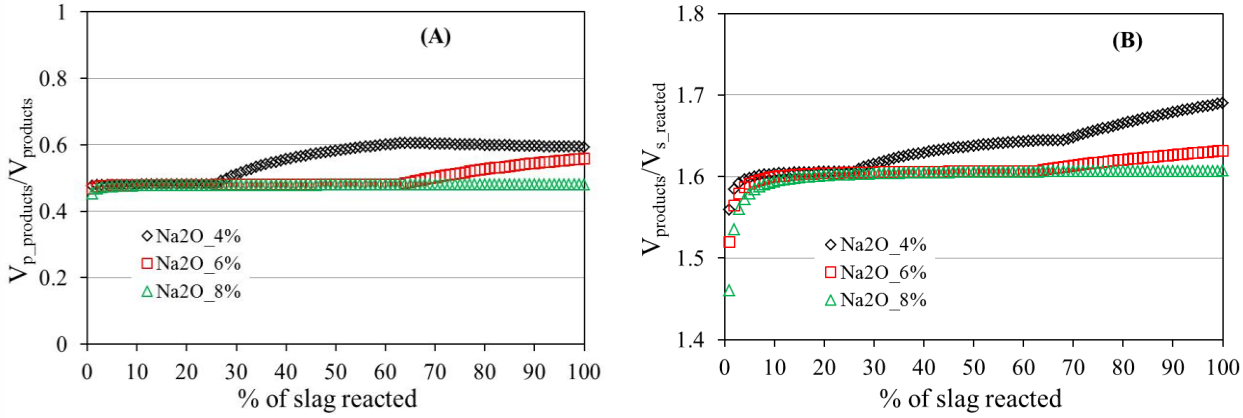

Figure 8: Volume fraction $V_{p\_products}/ V_{products}$ (A) and volume ratio $V_{products}/ V_{s\_reacted}$ (B).

Figure 8(A) shows that the volume fraction of primary products is between 40% and 60%, indicating that the primary reaction products and secondary reaction products contribute equally to the solid phase growth of alkali-activated slag. The volume fraction of primary products stays at 0.48 until slag reaction extent of 28% for Na_2O_4% and until 64% for Na_2O_6%. After those characteristic points of slag reaction extent, the volume fraction of primary products starts to increase slightly. For Na_2O_8%, the volume fraction of primary products almost remains at 0.48 during the whole slag reaction process.

The volume ratio ($V_{products}/ V_{s\_reacted}$) between the volume of products and the volume of reacted slag falls between 1.5 and 1.7, which is smaller than the value from 2.06 to 2.2 reported for Portland cement. [16] The volume ratio increases in the beginning and stays at 1.6 until slag reaction extent of 28% for Na_2O_4% and until 64% for Na_2O_6%. After those characteristic slag reaction extents the volume ratio increases gradually. For Na_2O_8%, the volume ratio also increases in the beginning until slag reaction extent of 8% and stays at 1.6 afterwards until complete slag reaction. The characteristic points of slag reaction extent of 28% and 64% for Na_2O_4% and Na_2O_6% in Figure 7(A) and Figure 8(A) correspond to the slag reaction extents when T2C* starts to appear in Figure 4 and Figure 5 respectively.

4 Conclusions

A newly developed thermodynamic approach was introduced to conduct a thermodynamic modeling study on the influence of NaOH on the phase assemblage and chemistry of aqeous solution in the alkali-activated slag paste (Na_2O/slag=4%, 6% and 8%). ICP-OES test was performed to investigate the chemistry of aqueous solution. Based on the finding results, the concluding remarks can be drawn:

(1) The calculated concentrations of elements in aqueous solution agree well with the experimental results. The concentrations of Na, OH^-, Si, Al, K and S increase with increasing content of Na_2O from 4% to 8% while the concentration of Ca shows an independence on the NaOH content.

(2) The uptake of Na into the primary reaction products decreases with slag reaction extent and increases with increament of NaOH content after a certain slag reaction extent. The

chemical shrinkage per gram of reacted slag is decreasing with increased NaOH content. Before slag reaction extent of 28%, the chemical shrinkage is independent of Na_2O content from 4% to 8%. After 28%, the influence of NaOH content on the chemical shrinkage depends on the slag reaction extent and NaOH content. The NaOH content does not have an obvious influence on the porosity development.

(3) In the calculated phase assemblage, T2C* and INFCN were produced as primary reaction products and OH-hydrotalcite, katoite, stratlingite, makinawite and portlandite were produced as secondary reaction products. The volume fraction of primary reaction products in total reaction products is between 40% and 60%, indicating equal contributions to solid phase growth between primary reaction products and secondary reaction products. The volume ratio between reaction products and reacted slag falls between 1.5 and 1.7, which is smaller than the value from 2.06 to 2.2 reported for Portland cement.

Acknowledgements

China Scholarship Council (CSC) and Microlab in Delft University of Technology are greatly appreciated for support in this research.

References

[1] Lothenbach, B.; Damidot, D.; Matschei, T.; Marchand, J.: Thermodynamic modelling: State of knowledge and challenges. *Advances in cement research* 22(4), pp.211-223, 2010.

[2] Damidot, D.; Lothenbach, B.; Herfort, D.; Glasser, F.P.: Thermodynamics and cement science. *Cement and Concrete Research* 41(7), pp.679-695, 2011.

[3] Lothenbach, B.; Gruskovnjak, A.: Hydration of alkali-activated slag: thermodynamic modelling. *Advances in cement research* 19(2), pp.81-92, 2007.

[4] Kulik, D.A.; Kersten, M.: Aqueous Solubility Diagrams for Cementitious Waste Stabilization Systems: II, End‐Member Stoichiometries of Ideal Calcium Silicate Hydrate Solid Solutions. *Journal of the American Ceramic Society* 84(12), pp.3017-3026, 2001.

[5] Myers, R.J.; Bernal, S.A.; Provis, J.L.: A thermodynamic model for C-(N-)A-S-H gel: CNASH-ss. Derivation and validation. *Cement and Concrete Research* 66, pp.27-47, 2014.

[6] Myers, R.J.; Lothenbach, B.; Bernal, S.A.; Provis, J.L.: Thermodynamic modelling of alkali-activated slag cements. *Applied Geochemistry* 61, pp.233-247, 2015.

[7] Barneyback Jr, R.S.; Diamond, S.: Expression and analysis of pore fluids from hardened cement pastes and mortars. *Cement and Concrete Research* 11(2), pp.279-285, 1981.

[8] Wolthers, M.; Charlet, L.; van Der Linde, P.R.; Rickard, D.; van Der Weijden, C.H.: Surface chemistry of disordered mackinawite (FeS). *Geochimica et Cosmochimica Acta* 69(14), pp.3469-3481, 2005.

[9] Kulik, D.A.; Wagner, T.; Dmytrieva, S.V.; Kosakowski, G.; Hingerl, F.F.; Chudnenko, K.V.; Berner, U.R.: GEM-Selektor geochemical modeling package: revised algorithm and GEMS3K numerical kernel for coupled simulation codes. *Computational Geosciences* 17(1), pp.1-24, 2013.

[10] Wagner, T.; Kulik, D.A.; Hingerl, F.F.; Dmytrieva, S.V.: GEM-Selektor geochemical modeling package: TSolMod library and data interface for multicomponent phase models. *The Canadian Mineralogist* 50(5), pp.1173-1195, 2012.

[11] Chen, W.; Brouwers, H.: The hydration of slag, part 1: reaction models for alkali-activated slag. *Journal of materials science* 42(2), pp.428-443, 2007.

[12] Lothenbach, B.; Matschei, T.; Möschner, G.; Glasser, F.P.: Thermodynamic modelling of the effect of temperature on the hydration and porosity of Portland cement. *Cement and Concrete Research* 38(1), pp.1-18, 2008.

[13] Haha, M.B.; Lothenbach, B.; Le Saout, G.; Winnefeld, F.: Influence of slag chemistry on the hydration of alkali-activated blast-furnace slag — Part I: Effect of MgO. *Cement and Concrete Research* 41(9), pp.955-963, 2011.

[14] Jensen, O.M.; Hansen, P.F.: Water-entrained cement-based materials: I. Principles and theoretical background. *Cement and Concrete Research* 31(4), pp.647-654, 2001.

[15] Myers, R.J.: Thermodynamic Modelling of CaO-Al2O3-SiO2-H2O-Based Cements. PhD thesis, University of Sheffield, Sheffield, 2015.

[16] Breugel, K.v.: Simulation of hydration and formation of structure in hardening cement-based materials. PhD thesis, Delft University of Technology, Delft, 1991.